

Gyrational modes of benzenelike magnetic vortex molecules

Christian F. Adolff,^{1,*} Max Hänze,¹ Matthias Pues,¹ Markus Weigand,² and Guido Meier^{1,3,4}

¹*Institut für Angewandte Physik und Zentrum für Mikrostrukturforschung, Universität Hamburg, 20355 Hamburg, Germany*

²*Max-Planck-Institut für Intelligente Systeme, Heisenbergstr. 3, 70569 Stuttgart, Germany*

³*The Hamburg Centre for Ultrafast Imaging, Luruper Chaussee 149, 22761 Hamburg, Germany*

⁴*Max Planck Institute for the Structure and Dynamics of Matter, Luruper Chaussee 149, 22761 Hamburg, Germany*

(Received 12 February 2015; revised manuscript received 7 July 2015; published 27 July 2015)

With scanning transmission x-ray microscopy we study six magnetostatically coupled vortices arranged in a ring that resembles a benzene molecule. Each vortex is contained in a ferromagnetic microdisk. When exciting one vortex of the ring molecule with an alternating magnetic high-frequency field, all six vortices perform gyrations around the equilibrium center positions in their disks. In a rigid particle model, we derive the dispersion relation for these modes. In contrast to carbon atoms, magnetic vortices have a core polarization that strongly influences the intervortex coupling. We make use of this state parameter to reprogram the dispersion relation of the vortex molecule experimentally by tuning a homogeneous and an alternating polarization pattern. In analogy to the benzene molecule, we observe motions that can be understood in terms of normal modes that are largely determined by the symmetry of the system.

DOI: [10.1103/PhysRevB.92.024426](https://doi.org/10.1103/PhysRevB.92.024426)

PACS number(s): 75.70.Kw, 02.20.-a, 68.37.Yz, 75.40.Gb

I. INTRODUCTION

In magnetic nanodisks of suitable geometry, the magnetization curls in the plane around the center of the disk and turns out-of-plane in the center. This magnetic ground-state configuration is called magnetic vortex. Dynamically, a gyration of the vortex core around the center of the disk is inherent in magnetic vortices [1]. Therefore it can be compared to a harmonic oscillator [2]. The polarization p , i.e., the out-of-plane direction of the vortex core ($p = \pm 1$), determines the gyration direction. It gyrates anticlockwise for positive polarization and clockwise for negative polarization. A second state parameter, the chirality ($C = \pm 1$), describes the sense of in-plane curling of the magnetization in the disk [3,4]. The gyrotropic mode can be resonantly excited in various ways, using magnetic fields or electric currents [5,6]. Vortices in coupled periodic arrangements feature properties that can be described with common concepts of solid state physics, i.e., group velocity, density of states, and band structure [7–9]. The coupling of vortices strongly depends on their relative polarizations. Thus arrangements of vortices are expected to feature a reprogrammable band structure depending on their polarization configuration [7,10–12]. The molecule benzene (C_6H_6) is a ring of six carbon atoms that each binds a hydrogen atom. When excited, for example, with infrared light, small vibrations of the atoms with respect to the interatomic distances emerge. Historically, the comprehension of the so-called normal modes and the relation to their excitation frequencies was crucial for understanding the infrared and Raman spectra. In this article, we study six magnetostatically coupled vortices arranged in a ring that resembles the benzene molecule. Scanning transmission x-ray microscopy is used to directly observe the gyrational excitations. We find that in analogy to the benzene molecule, normal modes explain the measured dynamics that largely depend on the symmetry of the

system. As for the actual benzene molecule, such symmetry considerations allow to understand the dynamics in a vivid fashion. The normal modes are plane waves with wavelengths that are fractions of the circumference of the ring, such as a breathing mode of the molecule. Our approach allows for deducing the dispersion relation of the vortex molecule in a convenient way. This will be shown in the last section. The dispersion relation depends on the tuned polarization states in the molecule and is measured for two states exemplarily.

II. NORMAL MODES OF VORTEX GYRATION

A convenient and powerful model to describe the motions of coupled vortices is the Thiele model [2,13–15]. It describes the magnetic vortex as a quasiparticle that is exposed to a force $\vec{F} = -\vec{\nabla}E$ that acts in the plane of the disk. In our case, it reads

$$(G_0^2 + D_0^2 \alpha_{\text{Gilbert}}^2) \dot{\vec{x}} = G_0 \tilde{r}_{90} \vec{F} - D_0 \alpha_{\text{Gilbert}} \vec{F}. \quad (1)$$

Here, \vec{x} is the two-dimensional position vector of the vortex core within the disk and \tilde{r}_{90} is a 90° rotation matrix. Two components add to the velocity of the vortex core. The first term describes the nature of the gyrotropic mode that moves the vortex perpendicular to the driving force \vec{F} . The second term depends on the dimensionless Gilbert damping parameter α_{Gilbert} and forces the vortex core back to its equilibrium position. The constants G_0 and D_0 depend on material parameters [2]. It can be challenging to determine the driving force \vec{F} in a coupled system. For a single magnetic vortex, a harmonic confining potential can be assumed to approximate the internal forces. A linear energy term is commonly used to describe the influence of external magnetic fields. Recent approaches for systems of vortices in coupled arrays employ surface charges that emerge when the vortex is deflected from the center of the disk to approximate the coupling mediated by the stray field [11,14–16]. Even when neglecting the damping, for a number of N coupled vortices, the Thiele equation becomes a $2N$ -dimensional system of differential

*adolff@physnet.uni-hamburg.de

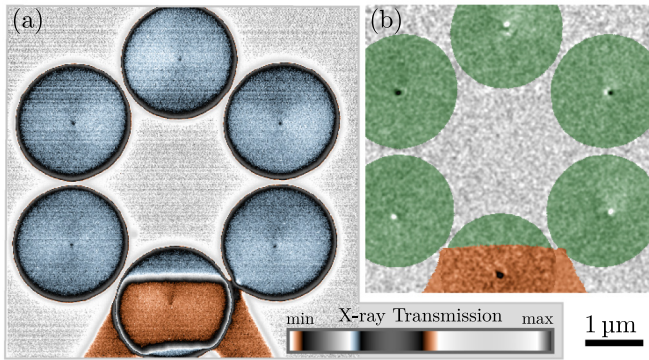


FIG. 1. (Color online) X-ray micrographs of six disks that contain a vortex each. The permalloy disks are 60-nm thick and have a 2- μm diameter, the minimal distance between the disks is 50 nm. (a) Vortex molecule with homogeneous core polarizations in all six disks. The magnetic contrast can be seen in the raw data of one time frame. The vortex cores appear as black dots. (b) Vortex molecule with alternating polarizations. The static contrast is subtracted to emphasize the magnetic contrast even more prominently. Disks and stripline are colorized. In the captured movie (see Ref. [18], movie 1) black vortex cores gyrate clockwise ($p_i = -1$) and white cores counterclockwise ($p_i = 1$).

equations that can only be solved numerically. Following the ideas of Wigner [17], we show that for rings of N coupled magnetic vortices the solution can be deduced exclusively by symmetry considerations. Figure 1 shows the investigated vortex molecule consisting of six permalloy ($\text{Ni}_{80}\text{Fe}_{20}$) disks.

A stripline is fabricated on one disk in order to excite the gyrotropic mode with the unidirectional high-frequency magnetic field generated by an alternating current sent through the stripline. The steady-state motions are directly observed by scanning transmission x-ray microscopy at the MAXYMUS microscope of the BESSY II synchrotron in Berlin, Germany. As can be seen in Fig. 1(b), the method provides magnetic contrast that allows to clearly see the vortex cores as white or black dots, corresponding to their polarization. The time resolution provided by the third generation synchrotron of up to 40 ps allows to trace the vortex trajectories (see Ref. [18], movies 1 and 3). In accordance with our measurements, we assume that the excitation will lead to approximately circular motions of the $N = 6$ vortices:

$$\vec{x}_i = a_i C_i \begin{pmatrix} \cos(\omega t + \varphi_i) \\ p_i \sin(\omega t + \varphi_i) \end{pmatrix}, \quad i \in \{0, 1, \dots, N-1\}. \quad (2)$$

With given chiralities C_i and polarizations p_i a motion of the molecule is fully determined by the N gyration amplitudes a_i and phases φ_i . In the experiment, the polarizations and the chiralities are measured [19]. Due to the N -fold rotational symmetry and the linearity of the system, there has to be a basis of N normal modes, that fulfill this symmetry. In analogy to the description of a linear chain of harmonic oscillators with periodic boundary conditions, we determine these modes to be plane waves with wavelengths that are fractions of the circumference of the ring. For a ring of an even number of N disks, the normal modes $\vec{x}_{i,\kappa}$ are given by

$$\vec{x}_{i,\kappa} \in \{\vec{x}_i \mid a_i = a_\kappa, \varphi_i = \varphi_{i,\kappa} = (\kappa + p_i) i \alpha + \phi_\kappa\}. \quad (3)$$

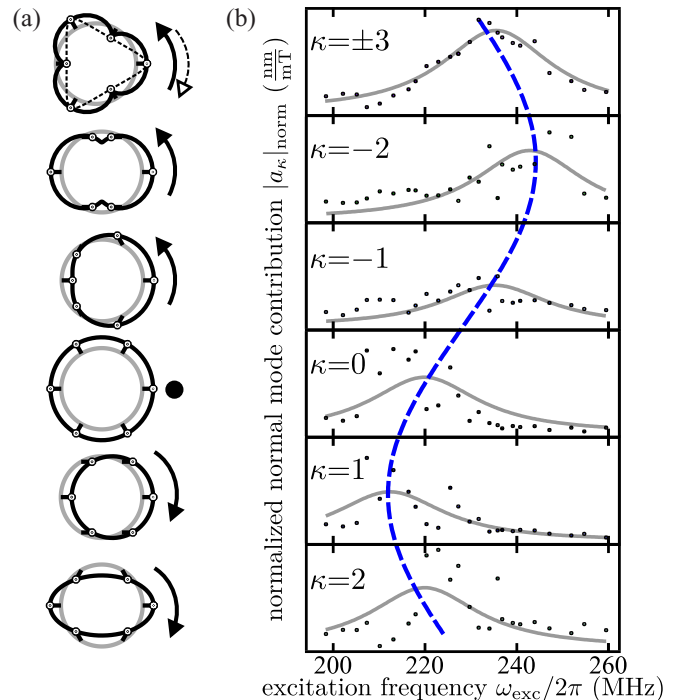


FIG. 2. (Color online) (a) Pictograms for the form and the propagation direction of the normal modes of the ring (see Ref. [18], movie 2). (b) Experiments with a homogeneous core polarization pattern in the ring ($p_i = -1$). Each graph shows the contribution of a normal mode to the overall motions in the molecule for different excitation frequencies. The data points are obtained by a fit to the trajectories traced via scanning transmission x-ray microscopy (see Fig. 1 and Ref. [18], movie 3). The solid lines are Lorentzian fit curves. The vertical scale of each graph ranges from 0 to 34 nm/mT.

The integer number $\kappa \in [-N/2, \dots, N/2)$ indexes the normal mode and is analogous to the wave number $k = 2\pi/\lambda$ in a linear chain of oscillators. The angle $\alpha = 2\pi/N$ corresponds to the lattice constant in a linear chain. Since a general vibration of the molecule is given by a linear combination of the normal modes $\vec{x}_i = \sum_\kappa \vec{x}_{i,\kappa}$, the factor a_κ describes the contribution of the normal mode $\vec{x}_{i,\kappa}$ to the motion. The relative phases of the normal modes are given by ϕ_κ . Figure 2(a) depicts the form of the normal modes for equal chiralities and polarizations ($c_i = 1, p_i = -1$) of all vortices. For each point in time, the vortex cores are located on geometric roulettes, i.e., epitrochoids and hypotrochoids. For wave numbers κ with $|\kappa| > 0$, the form of the roulettes stays constant over time and they rotate around the center of the ring, whilst the vortex cores are always located on the curve (see Ref. [18], movie 2). For positive wave numbers $\kappa > 0$, the roulettes rotate in the same direction as the vortices (clockwise). In contrast, for negative wave numbers, the roulettes rotate anti-clockwise, i.e., against the gyration direction of the vortices. Thus the sign of κ denotes the propagation direction of the waves. For $\kappa = 0$, the normal mode $\vec{x}_{i,0}$ is called the breathing mode since the vortices lie on a circle that changes its size over time. It can be compared to the modes 1 and 2 of the actual benzene molecule in the seminal work of Wilson, see Ref. [20], when only the vibrations of the carbon atoms are considered. At the edge of the Brillouin zone $\kappa = \pm 3$ the

waves can be understood as propagating in both directions. Figure 2(b) shows the experimental results for the investigated vortex benzene, when the homogeneous polarization pattern $p_i = -1$ is present. The steady-state motions of the vortices are traced for 24 different frequencies around the resonance frequency of an isolated disk. The grey line in each of the six graphs is a Lorentzian fit through the black data points that are proportional to the absolute gyration amplitude $|a_\kappa|$ of one normal mode $\vec{x}_{i,\kappa}$. These data points are obtained by applying a curve fit with the linear combination of normal modes given by Eqs. (2) and (3) to the vortex trajectories of the six vortices. In order to ensure a linear gyration regime, the amplitude of the excitation is adjusted to small vortex trajectories. The influence of different excitation strengths on the core velocity is normalized out [6,21]. For each frequency, one global curve fit is performed that comprises the complete motion of the six vortices and thus yields one data point in each of the six graphs. We point out that each eigenmode has its maximal contribution at different frequencies that lie on a sinusoidal line (dashed blue). Thus, contrary to the actual benzene molecule, the propagation of waves in the two possible directions (sign of κ) is not degenerated. The global rotation direction of the vortices in the homogeneous polarization case has no equivalent in the linear vibrations in benzene. Such kind of global gyration direction cannot be defined for an alternating polarization pattern since the vortices gyrate in different directions according to their polarization p_i . The alternating polarization pattern is shown in Fig. 1(b) and can be adjusted when a strong alternating magnetic field with a frequency of 224 MHz is applied via the stripline and is then reduced adiabatically. Although only one vortex is directly excited, this process of self-organized state-formation [16,23,29] allows to tune the polarizations in the whole molecule. The symmetry of the ring changes due to the alternating polarization pattern so that two normal modes $\vec{x}_{i,|\kappa|} = \vec{x}_{i,\kappa} + \vec{x}_{i,-\kappa}$ have to be combined in order to get standing waves. The combination of such standing waves is depicted in Fig. 3(a) (see also Ref. [18], movie 4). This time, all modes can be compared to the normal modes of the actual benzene molecule when only the carbon atoms are regarded. Using the Wilson numbering [20], the normal mode with $|\kappa| = 1$ corresponds to mode ‘‘Y’’ of the actual benzene, $|\kappa| = 2$ corresponds to mode ‘‘6a’’ and $|\kappa| = 3$ can be compared to normal mode ‘‘12.’’ The arrow pictograms in Fig. 3(a) are identical to those used by Wilson for the motions of the actual benzene. This elucidates the strong similarity between the actual benzene and vortex benzene. The standing waves are fitted to the trajectories and yield the results presented in Fig. 3(b) [28].

III. DISPERSION RELATION

Until now, we showed that there are strong similarities between the very different physical systems of magnetic vortices and bound carbon atoms with regard to their motions during a harmonic excitation. Both systems feature similar normal modes that are largely determined by the symmetry of the system. In the following, we will show that the symmetry considerations can be used to determine the dispersion relation of a ringlike vortex-molecule of arbitrary number of vortices in a very convenient way.

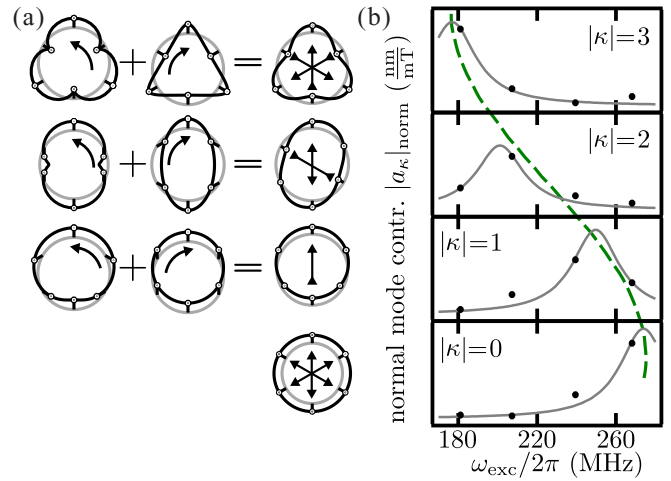


FIG. 3. (Color online) (a) Pictograms of the composition of the normal modes to obtain standing waves. (b) Experiments with alternating polarization pattern. Each graph shows the contribution of a standing wave to the overall motions in the molecule for different excitation frequencies. The data points are obtained by a fit to the trajectories traced via scanning transmission x-ray microscopy. The solid lines correspond to the fit with Eq. (10). The vertical scale is identical to that in Fig. 2.

To calculate the dispersion relation, we temporarily neglect the damping ($\alpha_{\text{Gilbert}} = 0$) in Eq. (1). All vortex trajectories are described by the $2N$ -dimensional vector $\vec{u} := (\vec{x}_0, \vec{x}_1, \dots, \vec{x}_{N-1})^T$ and each two-dimensional component of it follows Eq. (1). When a normal mode with circular trajectories $\vec{u}_\kappa = (\vec{x}_{0,\kappa}, \vec{x}_{1,\kappa}, \dots, \vec{x}_{N-1,\kappa})^T$ is inserted, it simplifies to

$$\omega_\kappa p \vec{u}_\kappa = \frac{1}{G_0} (\vec{F}_0, \vec{F}_1, \dots, \vec{F}_{N-1})^T. \quad (4)$$

\vec{F}_i describes the sum of all driving forces of vortex i . Multiplying both sides of the equation with \vec{u}_κ yields

$$\omega_\kappa = \frac{1}{p G_0} \frac{\sum_{i=0}^{N-1} \vec{F}_i \cdot \vec{x}_{i,\kappa}}{\sum_{i=0}^{N-1} \vec{x}_{i,\kappa}^2} = \frac{1}{p G_0} \frac{\sum_{i=0}^{N-1} \vec{F}_i \cdot \vec{x}_{i,\kappa}}{N a_\kappa^2}. \quad (5)$$

The driving forces \vec{F}_i are given by the total energy with respect to vortex i . We approximate the coupling between two vortices i and j by the most simple approximation, which is dipolar stray-field interaction [22]:

$$E_{\text{dipole},i,j} = \frac{\mu_0}{4\pi r^3} \left(\vec{\mu}_i \cdot \vec{\mu}_j - \frac{3}{r^2} (\vec{\mu}_i \cdot \vec{r})(\vec{\mu}_j \cdot \vec{r}) \right). \quad (6)$$

The dipole moment of a vortex is proportional to the deflection of the vortex rotated by 90 degrees ($\vec{\mu}_i = \tilde{r}_{90} C_i \tilde{a}_\kappa \vec{x}_{i,\kappa}$ [26]).

The strength of the dipole moment is denoted as \tilde{a}_κ since it is proportional to the gyration amplitude a_κ . For the given harmonic excitation, the chirality C_i has no influence on the dipole moment, since the change of sign is compensated by a phase shift of 180° in time. The anchor points of the dipoles are assumed to be fixed at the centers of the disks. Thus, the vector \vec{r} , that connects the dipoles, is constant. Separating the dipolar coupling from all other forces that act on the isolated

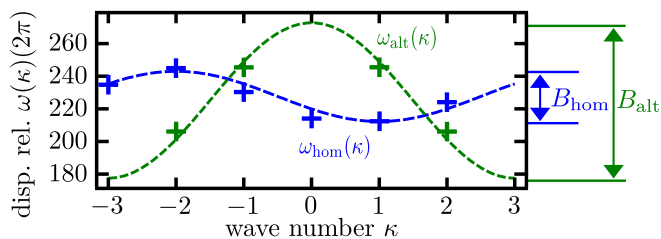


FIG. 4. (Color online) Experimentally determined dispersion relations for the two polarization patterns and theoretical fit curves derived from the extended Thiele model. The dashed lines result from a global curve fit of Eq. (10). The data points result from individual Lorentzian curve fits to the experimental results.

disks yields

$$\omega_{\kappa} - \omega_0 = -\frac{1}{p} \frac{1}{G_0} \frac{1}{N a_{\kappa}^2} \sum_{i=0}^{N-1} \sum_{j \neq i} E_{\text{dipole},i,j}. \quad (7)$$

The resonance frequency ω_0 applies for noninteracting vortices in isolated disks. Only considering next-neighbor interaction yields the discrete dispersion relation [27]

$$\omega_{\text{hom}}(\kappa) = \omega_0 - \frac{1}{2} B_{\text{hom}} \cos((\kappa + p)\alpha) \quad (8)$$

for the homogeneous case. For the alternating polarization pattern, it is useful to integrate Eq. (7) over one period of gyration to separate ω_{κ} . It then yields

$$\omega_{\text{alt}}(\kappa) = \omega_0 + \frac{1}{2} B_{\text{alt}} \cos(\kappa\alpha), \quad B_{\text{alt}} = 3 B_{\text{hom}}, \quad (9)$$

for the alternating polarization pattern. The bandwidth B_{hom} is a positive constant given by $B_{\text{hom}} = \frac{-1}{p G_0} \frac{\mu_0}{4\pi r^3} \left(\frac{\tilde{a}_{\kappa}}{a_{\kappa}}\right)^2$. When comparing the two analytically calculated dispersion relations ω_{alt} and ω_{hom} , one can see that the factor p has vanished in the cosine and that the prefactor is multiplied by (-3) . The different bandwidths are commonly explained by a weaker coupling between vortices of equal polarization than of vortices with different polarizations [24]. For the borderline case of an infinite linear chain ($N \rightarrow \infty$), the results are in concordance with previous results [11]. In the following, we include the effects of damping and the experimental results. For negligible damping, there are sharp resonances when the eigenfrequency of a normal mode is met. In the experiment, the damping allows to excite the system in between those resonances. The normal modes mix in the way shown in Fig. 2 (also see Ref. [18], movie 3). The contributions $a_{\kappa}(\omega_{\text{exc}})$ are fitted to the experimental data with Lorentzian functions that are shifted according to the analytically derived discrete dispersion relation $\omega(\kappa)$:

$$a_{\kappa}(\omega_{\text{exc}}) = \mathcal{L}_{\Gamma}(\omega_{\text{exc}} - \omega(\kappa)), \quad \kappa \in [-N/2, \dots, N/2]. \quad (10)$$

This set of equations can be understood as the continuous dispersion relation of the damped system, where ω_{exc} is the frequency of the exciting magnetic field and $\mathcal{L}_{\Gamma}(\omega)$ the Lorentzian peak function with damping parameter Γ . The

fit yields the three model parameters ω_0 , B_{hom} , and Γ . The first two parameters determine the discrete dispersion relations shown in Fig. 4. The dashed green [blue] curve corresponds to the dispersion relation $\omega_{\text{alt}}(\kappa)$ [$\omega_{\text{hom}}(\kappa)$] measured for the alternating [homogeneous] polarization configuration of the vortex molecule. The data points correspond to peaks of individual Lorentzian fits as presented in Fig. 2(b). The parameters are determined to be $\omega_0/2\pi = (225.5 \pm 1.5)$ MHz and $B_{\text{alt}} = (96 \pm 6)$ MHz for the alternating case and $\omega_0/2\pi = (227.6 \pm 0.8)$ MHz and $B_{\text{hom}} = (31 \pm 2)$ MHz for the homogeneous polarization pattern. Those are appropriate values for the bandwidth when considering the low disk interdistance [30]. In both cases, the damping parameter has a value of $\Gamma = (29 \pm 3)$ MHz, which is in reasonable accordance with the relation $\Gamma = 2\alpha_{\text{Gilbert}}\omega \approx 0.02 \omega$ expected from other studies [32].

IV. CONCLUSION

In conclusion, we have shown that there are strong similarities between the vibrational modes of benzene and the gyration modes of a sixfold magnetic-vortex ring molecule. The symmetry of both systems determines the motions of the oscillators, i.e., the carbon atoms or the vortices. The best accordance in the analogy can be achieved when an alternating polarization pattern is tuned to the vortex molecule. In this case, all gyration modes can be identified with vibrational modes in the actual benzene. The symmetry allows to simplify the derivation of the fundamentally different dispersion relations of the vortex molecule for the homogeneous and alternating core polarization patterns. In contrast to other models, the presented approach includes the effect of damping and is characterized by only three model parameters, each of them determined in the experiments. Both dispersion relations have been confirmed by x-ray transmission microscopy proving that the magnetic vortex molecule features a reprogrammable band structure or dispersion relation.

ACKNOWLEDGMENTS

We thank Ulrich Merkt for fruitful discussions, Benedikt Schulte for support during the evaluation of the measurements, and Michael Volkmann for superb technical assistance. We acknowledge the support of the Max-Planck-Institute for Intelligent Systems (formerly MPI for Metals Research), Department Schütz and the MAXYMUS team, particularly Michael Bechtel and Eberhard Goering. We thank the Helmholtz-Zentrum Berlin (HZB) for the allocation of synchrotron radiation beamtime. Financial support of the Deutsche Forschungsgemeinschaft via the Sonderforschungsbereich 668 and the Graduiertenkolleg 1286 is gratefully acknowledged. This work has been supported by the excellence cluster “The Hamburg Centre for Ultrafast Imaging - Structure, Dynamics, and Centre of Matter at the Atomic Scale” of the Deutsche Forschungsgemeinschaft.

[1] S.-B. Choe, Y. Acremann, A. Scholl, A. Bauer, A. Doran, J. Stöhr, and H. A. Padmore, *Science* **304**, 420 (2004).

[2] B. Krüger, A. Drews, M. Bolte, U. Merkt, D. Pfannkuche, and G. Meier, *Phys. Rev. B* **76**, 224426 (2007).

- [3] T. Shinjo, T. Okuno, R. Hassdorf, K. Shigeto, and T. Ono, *Science* **289**, 930 (2000).
- [4] A. Wachowiak, J. Wiebe, M. Bode, O. Pietzsch, M. Morgenstern, and R. Wiesendanger, *Science* **298**, 577 (2002).
- [5] B. Van Waeyenberge, A. Puzic, H. Stoll, K. W. Chou, T. Tyliczszak, R. Hertel, M. Fähnle, H. Brückl, K. Rott, G. Reiss, I. Neudecker, D. Weiss, C. H. Back, and G. Schütz, *Nature (London)* **444**, 461 (2006).
- [6] T. Kamionka, M. Martens, A. Drews, B. Krüger, O. Albrecht, and G. Meier, *Phys. Rev. B* **83**, 224424 (2011).
- [7] V. V. Kruglyak, S. O. Demokritov, and D. Grundler, *J. Phys. D: Appl. Phys.* **43**, 260301 (2010).
- [8] B. Lenk, H. Ulrichs, F. Garbs, and M. Münzenberg, *Phys. Rep.* **507**, 107 (2011).
- [9] S.-K. Kim, *J. Phys. D: Appl. Phys.* **43**, 264004 (2010).
- [10] M. Krawczyk and D. Grundler, *J. Phys.: Condens. Matter* **26**, 123202 (2014).
- [11] D.-S. Han, A. Vogel, H. Jung, K.-S. Lee, M. Weigand, H. Stoll, G. Schütz, P. Fischer, G. Meier, and S.-K. Kim, *Sci. Rep.* **3**, 2262 (2013).
- [12] C. Behncke, M. Hänze, C. F. Adolff, M. Weigand, and G. Meier, *Phys. Rev. B* **91**, 224417 (2015).
- [13] A. A. Thiele, *Phys. Rev. Lett.* **30**, 230 (1973).
- [14] J. Shibata, K. Shigeto, and Y. Otani, *Phys. Rev. B* **67**, 224404 (2003).
- [15] M. Hänze, C. F. Adolff, M. Weigand, and G. Meier, *Appl. Phys. Lett.* **104**, 182405 (2014).
- [16] C. F. Adolff, M. Hänze, A. Vogel, M. Weigand, M. Martens, and G. Meier, *Phys. Rev. B* **88**, 224425 (2013).
- [17] E. Wigner, *Nachrichten d. Gesell. d. Wissenschaften z. Göttingen, Math.-Phys., Klasse* **1**, 133 (1930).
- [18] See Supplemental Material at <http://link.aps.org/supplemental/10.1103/PhysRevB.92.024426> for the supplemental movies and movie descriptions.
- [19] In order to determine the chiralities, a different setting of the microscope is used that provides in-plane contrast.
- [20] E. B. Wilson, *Phys. Rev.* **45**, 706 (1934).
- [21] T. J. Silva, C. S. Lee, T. M. Crawford, and C. T. Rogers, *J. Appl. Phys.* **85**, 7849 (1999).
- [22] A. Vogel, A. Drews, T. Kamionka, M. Bolte, and G. Meier, *Phys. Rev. Lett.* **105**, 037201 (2010).
- [23] S. Jain, V. Novosad, F. Y. Fradin, J. E. Pearson, V. Tiberkevich, A. N. Slavin, and S. D. Bader, *Nat. Commun.* **3**, 1330 (2012).
- [24] A. Vogel, T. Kamionka, M. Martens, A. Drews, K. W. Chou, T. Tyliczszak, H. Stoll, B. Van Waeyenberge, and G. Meier, *Phys. Rev. Lett.* **106**, 137201 (2011).
- [25] J. Mejía-López, D. Altbir, A. H. Romero, X. Batlle, I. V. Roshchin, C.-P. Li, and I. K. Schuller, *J. Appl. Phys.* **100**, 104319 (2006).
- [26] This is a simplification of the model commonly used to describe the stray-field coupling of magnetic vortices. It corresponds to an analytical expression for the numerical coupling integrals described in Refs. [14,31], i.e., $\eta_{xx} \propto (\frac{1}{r^3} - \frac{3r_y^2}{r^5})$, $\eta_{yy} \propto (\frac{1}{r^3} - \frac{3r_x^2}{r^5})$, $\eta_{xy} = \eta_{yx} \propto \frac{3r_x r_y}{D^5}$, whereas the vector $\vec{r} = (r_x, r_y)^T$ connects the centers of two disks.
- [27] It is straightforward to include the interaction between all neighbors, but due to the large distance of the disks this is a small correction that can be neglected here [22,25].
- [28] Due to the limited beam time, the chiralities of the vortices have not been measured for the alternating case. They are determined to fit best with $C_i = (-1, 1, 1, -1, 1, 1)^T$.
- [29] M. Hänze, C. F. Adolff, M. Weigand, and G. Meier, *Phys. Rev. B* **91**, 104428 (2015).
- [30] S. Sugimoto, Y. Fukuma, S. Kasai, T. Kimura, A. Barman, and Y. C. Otani, *Phys. Rev. Lett.* **106**, 197203 (2011).
- [31] J. Shibata and Y. Otani, *Phys. Rev. B* **70**, 012404 (2004).
- [32] M. Martens, T. Kamionka, M. Weigand, H. Stoll, T. Tyliczszak, and G. Meier, *Phys. Rev. B* **87**, 054426 (2013).